Design of pin connections between steel members

Jorge Conde [a],[*], Luis S. da Silva [b], Trayana Tankova [c], Rui Simões [b], Tiago Abecasis [d]

[a] *Universidad Politécnica de Madrid, Departamento de Física y Estructuras de Edificación, Av. Juan de Herrera, 4, 28040 Madrid, Spain*
[b] *University of Coimbra, ISISE, Department of Civil Engineering, Portugal*
[c] *Technical University Delft, Department of Civil Engineering, the Netherlands*
[d] *Tal Projecto, Portugal*

ARTICLE INFO

ABSTRACT

The design of pin connections between steel members has been established for many years in design codes. However, recently, in the scope of the revision of Eurocode 3, Part 1–8 (EN 1993–1-8), questions were raised concerning the safety of the corresponding design verifications. This paper identifies two main aspects that require revision, namely: (i) the possibility to design a pin as a bolt in shear and (ii) the verification of the resistance of the pin itself. Based on a thorough literature review, experimental tests and a parametric study, a new proposal submitted to CEN as an amendment to the code, is presented to solve these two identified issues.

1. Introduction

Pin connections are used extensively in civil and mechanical engineering for the direct materialization of a 2D simple support (external restraint) or a perfect hinge (internal constraint). The connection is formed by a central steel rod (the pin), with its axis perpendicular to the applied load, and several plates (the lugs, either supporting or supported) with circular holes through which the pin is inserted. Fig. 1 shows a typical pin detail.

Retainer elements are fixed to both extremities of the pin to prevent it from sliding out of the connection. These elements, however, are not covered by current code specifications and are disregarded in design. Tolerance gaps between plates can be provided to facilitate erection and reduce friction. The plates are generally considered to be in a state of planar stress and the supporting ones will contact the pin on the cylindrical surface opposite to the supported ones. If the connected plates are thick (a thickness approaching the pin diameter) this assumption is only approximate. It is generally assumed that the connection presents high rotational capacity, although this aspect has not been proven experimentally.

Recently, in the scope of the ongoing revision of the structural Eurocodes, questions were raised concerning the safety of the design provisions of pin connections currently stated in EN 1993–1-8 [1], hereby referred to as EC3–1-8. These concerns led to the preparation of an amendment to EC3–1-8 to correct this safety issue. It is the objective of this paper to provide a background for the design of pins that supports

the adoption of the amendment.

Firstly, a detailed literature review is presented. Then, the specifications in EC3–1-8 are summarized. Subsequently, the results of an experimental testing program are reported and compared with the current code specifications, followed by an extensive parametric study addressing the limits of application of the current EC3–1-8 specifications. Finally, a new proposal for the design of pins is derived and presented.

2. Literature review

2.1. Geometry

Eye bars for chains in suspension bridges can be regarded as pin connections. In this context, Winkler (reported in [2]) proposed a geometry that has been adopted as the basis for pin design in EC3–1-8 (see Table 3.9 of the standard) and will likely be maintained in the next revision of this code. This geometry is shown in Fig. 2(a) in comparison with the EC3–1-8 'Type A' geometry shown in Fig. 2(b) (EC3–1-8 'type B' geometry results in a similar figure). In this figure, b is the minimum width based on yield strength, that is

$$b = \frac{F_{Ed}}{t f_y / \gamma_{M0}}, \tag{1}$$

where F_{Ed} is the design axial force, t is the lug thickness, f_y is the yield stress and γ_{M0} the partial factor generally recommended as 1. It is worth

* Corresponding author.
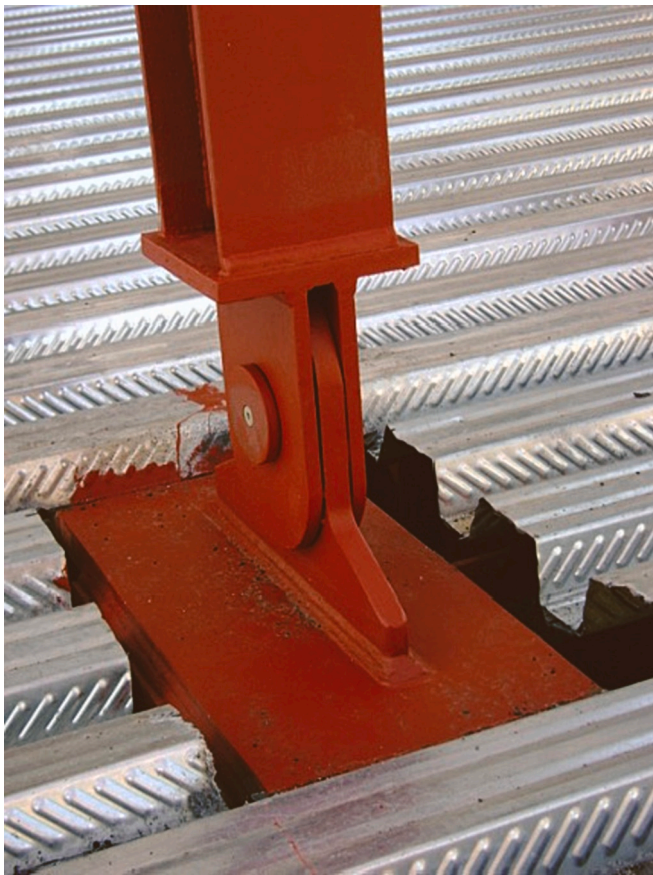*E-mail address:* jorge.conde@upm.es (J. Conde).

Fig. 1. Pin detail (New General Hospital, Toledo, Spain; courtesy of V. Ríos).

mentioning that this geometry was proposed strictly for tension loads acting along the symmetry axis of the lug; therefore, the code geometry is not intended for use in simple supports (in which the reactions might adopt different directions depending on lateral forces, and the plates are mainly in compression) or internal hinges (which are generally subjected to shear and axial forces). Lug geometries with non-parallel lateral surfaces are more suitable for these cases but are not covered by EC3–1-8. In common practice, loads at different angles are possible. Melcon and Hoblit [3] performed some tests on pin connections transversally loaded for closely fitting pins and presented empirical resistance curves. Ekvall [4] analysed the case of load applied at 45° and 90° from the axis of symmetry, reporting stress concentration factors up to 15% larger than for load applied at 0° (load parallel to the plate axis). This analysis was carried out on plates not compliant with EC3–1-8 geometrical specifications (lugs with lateral surfaces forming a 90° angle).
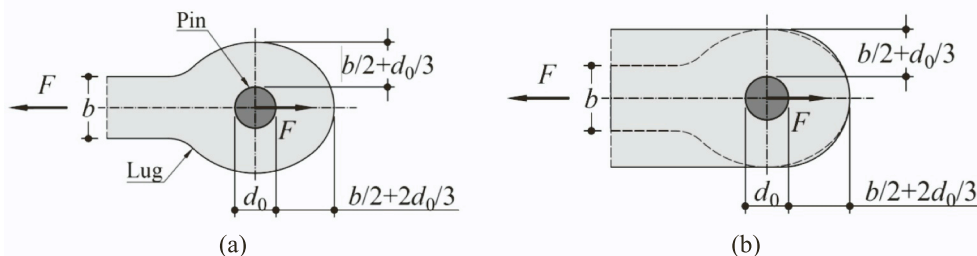
2.2. Elastic behaviour

The elastic behaviour of the plates, particularly the contact stress distribution between pin and lugs, was first studied by Hertz [5] and subsequently by different authors [6–11]; detailed reviews can be found in [12,13]; stress concentration factors have been studied using analytical, numerical and experimental techniques (particularly photoelasticity); different analytical studies reach different conclusions depending upon the initial assumption of stress distribution on the pin. This distribution is highly influenced by the clearance between pin surface and hole [14–16] and by the external geometry of the lug [17]. Stress concentration factors were an important topic for aircraft design before the introduction of FEM. For structures, this topic is particularly relevant for serviceability (a verification neglected for non-replaceable pins in EC3-1-8). Duerr [18] used data from different studies to propose an empirical expression for the stress concentration factor, assuming that certain geometrical conditions of plate and pin are fulfilled. When applied to EC3-1-8 geometry (configuration type B, see Table 3.9 in the standard), Duerr's expression predicts a stress concentration factor of 3.22 (related to the average tensile stress on the net plate area). The influence of the different materials on the stress concentration factors is briefly treated in [19] and found to be negligible if the ratio of elastic moduli between pin and plate is between 1 and 3; this is of no consequence for connections with steel pin and plates where this ratio is approximately 1. Furthermore, as pointed out by Johnston [14], for a ductile material (such as structural steel), elastic stress concentrations have a negligible effect on the ultimate strength of the connection and a very limited effect on the overall elastic deformation. Thus, they are not critical for design and are not discussed further in this paper.

2.3. Ultimate behaviour

2.3.1. Introduction

The ultimate behaviour of pin connections has been studied experimentally (Johnston, 106 tests [14]; Luley, 16 tests [20]; Melcon and Hoblit, 30 tests [3]; Tolbert and Hacket, 13 tests [8]; Blake, 23 tests [21]; Duerr and Pincus, 13 tests [22]; Bridge et al., 18 tests [23]; Rex and Easterling, 48 tests [24]) and numerically [12,25]. Based on experimental results, some authors have proposed design expressions. The most relevant are qualitatively discussed below. The range of specimens studied in the cited references is between the following values: plate thickness between 3 mm–50 mm; pin diameter between 12.7 mm–76.2 mm. Most of the studies deal with the failure modes of lugs, and only a few works tackle the pin strength and deformation. This lack of experimental data could become critical in the current construction scenario, where the use of high strength steel is becoming common, and the pin might no longer be the strongest element in the connection [26].

2.3.2. Failure modes

Eye bars with pins have been the subject of different empirical studies; the largest and most important one was carried out by Johnston [14], who studied 106 specimens of elongated steel plate links loaded

Fig. 2. Lug geometry: (a) adapted from Winkler; (b) adapted from EC3–1-8 ('Type A' geometry).

along their symmetry axis by means of 73.5 mm steel pins inserted in bored holes at either end of the plate, with squared or chamfered plate ends. Plate thickness was within 3 mm–19 mm, plate width between 152 mm–254 mm, edge distance behind pinhole between 25 mm–81 mm and pin clearance between tight fit and 5 mm. Fig. 3(a) shows the type of plates included in the tests. The range of the study was further enlarged by Blake [21] to plates of up to 50.8 mm thickness (this author barely presented test results, without interpreting them or deriving any analytical expression). Johnston proposed semi-empirical equations to estimate the ultimate plate strength, distinguishing four failure modes for the plates, see Fig. 3(b): 1) plate tension failure in net section through hole; 2) plate splitting beyond the pin; 3) plate shearing beyond the pin; 4) plate 'dishing' (out of plane instability due to compression exerted by the pin surface on the plate). Modes 2 and 3 are not clearly separated in the original work, but Duerr [18] proposed to treat them as different failure modes. Interestingly, none of these failure modes is directly addressed in the current version of EC3–1-8. However, the code contemplates three additional modes regarding the pin strength: 5) pin bending failure; 6) pin shear failure, and 7) pin bending-shear interaction. The code also includes verifications for 8) bearing resistance and 9) maximum contact stress. The latter is only applied to replaceable pins. Mode 8 is obviously related to modes 2 and 3, including them implicitly as a function of the end distances [27].

2.3.3. Discussion of plate failure modes

Regarding mode 1 (tension failure resistance at net section), Duerr [18] proposed a method for the calculation of tension failure resistance, based both on stress concentration factors and experimental data obtained in [14,22]. The method is based on an effective net area (smaller than the actual net area). Application of the method to EC3–1-8 geometrical configuration (see Table 3.9 in the standard) results in an effective tensile area of about 76% to 100% of the actual net area, depending on the material of the plate. Additional reduction is necessary to account for hole clearance, as discussed below.

For mode 2 (plate splitting beyond hole), an empirical equation has been proposed in [14], based on the results of 23 tests, validated and extended with additional tests by other authors ([8,21,22,24]). Hole clearance results, again, in capacity reduction. For the EC3–1-8 configuration with closely fit pins, this mode of failure is not critical.

According to [18], mode 3 (plate shearing beyond the hole) can be addressed with a block tearing verification with double shear. However, based on tests, this author proposes to use ultimate shear strength instead of the conventional value of yield shear strength. Depending on the value adopted, this verification could become critical for the EC3–1-8 configuration.

Out-of-plane instability (mode 4) is likely to occur only for slender plates. The stress distribution around the pin includes local compression components, even if the plate is subjected to tensile stress. Johnston [14] proposed an empirical equation to predict this phenomenon. However, further tests in [24] showed that the equation was inaccurate. Instead, Duerr [18] proposed a verification method based on column buckling theory, assimilating the plate beyond the pin to a cantilevered column

with a correction for the panel aspect. The verification can be skipped if the plate slenderness is below a certain limiting value; this check is not directly included in EC3–1-8.

The effect of pin-hole clearance (disregarded in the current EC3–1-8 formulation) has been studied experimentally [28] (referenced in [15]), and analytically, [11,25], and found to be of importance both for ultimate load capacity and stress concentration factor. A maximum hole-diameter-to-pin-diameter ratio of 1.1 has been suggested in [15]. For plates fulfilling the Eurocode 3 geometrical requirements, this limit results in an approximate increase of 10–20% in the stress concentration factor. However, no specific rules regarding hole tolerances for pin connections are included in EC3–1-8. Limited experimental data [8] are available for larger clearances.

2.3.4. Discussion of pin failure modes

Pin bending strength (modes 5, 6 and 7) is treated in some experimental and theoretical papers, [3,29] (reported in [13]), [30]; these works are summarized in [13] concluding that: i) there is a lack of experimental data on large diameter pins; ii) there are different approaches to characterize the distribution of bearing stresses along the length of the pin (stress distribution models), but no actual data is available to support these formulations. Despite the absence of pin failures in tests, Melcon and Hoblit [3] discussed the importance of the pin strength and stiffness for the overall behaviour, arguing that their lack of strength and stiffness can precipitate lug failure. Moreover, these authors indicate that the clamping effect due to retainer plates must be disregarded, and discussed the effect of pin stiffness and bending strength on the connection capacity, proposing a model in which the plate forces are applied to the pin as uniformly distributed along the length in contact and the pin internal forces are calculated using simple beam theory; this is the model implemented in EC3–1-8. However, the authors explicitly indicate that this is only valid for stiff (stout) pins, defined as those presenting negligible permanent deformation after the load is retired. The load distribution can be intuitively explained by imagining each individual lug as formed by independent laminations: for slender pins likely to present large bending curvature, only some laminations will contact the pin and carry the load, and their rupture strain might be reached before all other laminations are engaged. For strong and stiff pins, the load must be distributed uniformly for external plates (for equilibrium), whereas for internal plates the load can be uniformly distributed along the plate thickness or concentrated on a certain length of the external edges, to be calculated according to a procedure presented by these authors. Blake [29] (reported in [13]) proposed to find the internal forces with a 4-point bending model, in which the point load on the central plate is applied as two equal forces at one-quarter and three-quarters of its thickness, and the point load on the external plates is applied at its centreline; this model with concentrated loads results in higher bending moments and might be too conservative.

2.3.5. Moment-shear interaction at the pin

The pin design resistance can be obtained by the usual strength of materials formulae for circular cross-sections. EC3–1-8 defines the
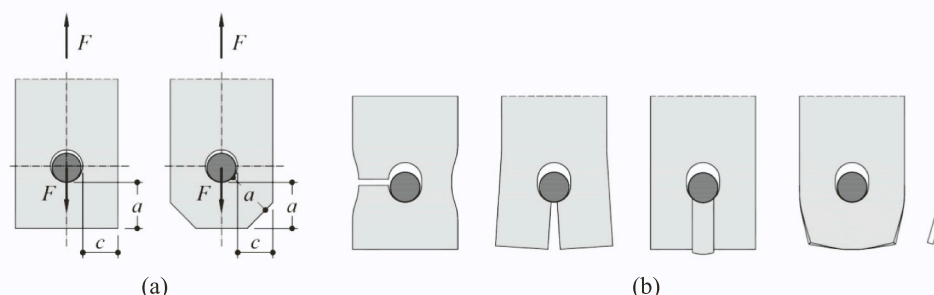

Fig. 3. Tests by Johnston [14]: (a) Specimen geometry; (b) Failure modes (from left to right, tension failure, plate splitting, plate shearing, plate dishing).

bending resistance M_{Rd} (mode 5) as 1.5 times the elastic bending resistance $M_{\text{el,Rd}}$ for the circular solid section. The shear resistance $F_{\text{v,Rd}}$ (mode 6) defined in the code is 0.6 times the tensile strength, which corresponds approximately to the Von Mises criterion applied using tensile stress instead of yield stress. Bending moment-shear interaction (mode 7) is verified with an expression of the type

$$\left(\frac{M_{\text{Ed}}}{M_{\text{Rd}}}\right)^a + \left(\frac{F_{\text{v,Ed}}}{F_{\text{v,Rd}}}\right)^b \leq 1, \tag{2}$$

where M_{Ed} and $F_{\text{v,Ed}}$ are, respectively, the design internal bending moment and shear force at the same cross-section along the pin axis; and $a = b = 2$; this expression is exact if perfect plasticity is assumed. It is worth mentioning that by the EC3–1-8 approach, a strictly designed pin is likely to start yielding even at the Serviceability Limit State (SLS), due to the proportion between design loads at Ultimate Limit State (ULS) and SLS being necessarily <1.5. The pin bending-shear interaction proposal in [30] differs from the European standard in the following aspects: i) moment resistance is based on plastic moment resistance (which is approximately 1.7 times the elastic moment resistance); ii) shear resistance is based on yield strength and Von Mises criterion; iii) the interaction formula, Eq. (2), is applied with $a = 1$, $b = 3$, and the unity in the second member is reduced to 0.95; because maximum bending moment appears at zero shear force, the last condition results in an actual moment resistance approximately 1.6 times the pin elastic moment resistance.

2.4. Deformation

The deformation of pin connections has been experimentally and numerically studied by different authors [14,21,22,24]. Measurement points and methods differ between studies, so a comparison of results is not possible. A method to find the plate stiffness of the pin connection has been proposed in [24] and later modified in [18], but only for hole-diameter-to-pin-diameter ratios up to 1.1. However, the model contemplates a square plate geometry not compatible with EC3–1-8 geometrical requirements, is limited to values of bearing deformation of about 0.25 mm and is not validated for very close-fitting pins (pins with very small clearances), widespread in common practice.

2.5. Conclusions of the literature review

This literature review shows that significant gaps in the knowledge of pin connections exist. In particular:

- Many tests have been carried out on pin connections; however, most of them have been performed on specimens conforming to eye bars (rectangular lugs) with symmetrical load; most of the experiments and analytical studies focus on plate behaviour.
- The influence of the pin slenderness and its effect on the overall connection behaviour is not well tested and studied.
- Current empirical expressions to estimate the strength of the connection have been derived for conventional mild steel lugs, with the plate material always weaker than the pin material and largely ductile; increasing use of high-strength steel, with inherent reduced ductility, suggests a need for empirical validation of lugs manufactured in this material.
- There is a lack of experimental data for complex geometries (such as lugs with non-parallel sides) and load situations (different load orientations). Pin connections with >3 lugs, common in practice, are not specifically addressed and tested in the literature.

Regarding the EC3–1-8 design recommendations for pins, the following conclusions can be stated:

- The EC3–1-8 proposal for the design of pin elements is very limited. In its current state, it is only suitable for tension elements with symmetrical load and does not include verifications for some of the limit states treated in the literature.
- The effect of hole clearance is not included in the code; however, experiments have shown that it results in a considerable decrease in overall strength.
- Strict design of the pin according to the code results in partial yielding at the serviceability limit state, which is contrary to the design concept generally adopted on other parts of the Eurocode.
- The possibility to design the pin as a bolt is in direct conflict with the absence of a clamping effect and is therefore unsafe.
- The possibility of accidental asymmetry in the central plate position (due to the gap between plates) is not contemplated in the code.

The last two points are discussed in detail in the following sections, and corresponding amendments to the EC3–1-8 text are proposed.

3. Eurocode provisions for the design of pin-connected joints in tension

For pin connections where free rotation is required, with the geometry of plates in accordance with the dimensional requirements given in Table 3.9 of EC3–1-8, the code provisions for the design of plates and pins are described in Table 1, Eqs. (3) to (8):

In Table 1, A is the cross-sectional area of the pin; d is the diameter of the pin; t is the thickness of the connected part; W_{el} is the flexural elastic modulus of the pin; f_y is the lower of the yield strengths of the pin and the connected part; f_{up} is the ultimate tensile strength of the pin; f_{yp} is the yield strength of the pin; γ_{M0}, γ_{M2}, $\gamma_{\text{M6,ser}}$ are partial factors with recommended values $\gamma_{\text{M0}} = 1.0$; $\gamma_{\text{M2}} = 1.25$, $\gamma_{\text{M6,ser}} = 1.0$.

The relation between the bending moment (M_{Ed}) in the pin and the applied force (F_{Ed}) is obtained as indicated in Fig. 4. The elastic and plastic modulus of a solid circular section are, respectively, $W_{\text{el}} = \pi \cdot d^3 / 32$ and $W_{\text{pl}} = d^3/6$, with a shape factor $W_{\text{pl}}/W_{\text{el}} \approx 1.7$. Therefore, the code bending resistance ($1.5 \cdot W_{\text{el}}$) is between the elastic and plastic resistance. The shear resistance is purely plastic and based on the ultimate tensile strength. It is worth mentioning that, if the design exhausts the code bending resistance at ULS, the pin will likely enter the plastic range in SLS. Due to the nature of the problem (few connections with a large responsibility), it might be reasonable to adopt a more conservative approach, which could be easily done by replacing the coefficient 1.5 with 1.35 in Eq. (6).

In addition, clause 3.14.1(2) of EC3-1-8 states that pin connections in which no rotation is required may be designed as single bolted connections, provided that the length of the pin is <3 times the diameter of the pin. Otherwise, pin connections should be designed using the method given in clause 3.13.2 of the cited code. A simple counterexample can prove that application of this rule leads to unsafe results: consider a pin connection as described in Fig. 4, with all elements in steel grade S355 ($f_y = 355$ MPa, $f_u = 510$ MPa), pin diameter $d = 16$ mm,

Table 1
Design resistance of pin connections (adapted from Table 3.9 of EC3-1-8).

| Failure mode	Expression	
Shear resistance of pin	$F_{\text{v, Rd}} = 0.6 A f_{\text{up}}/\gamma_{\text{M2}}$	(3)
Bearing resistance of plate and pin	$F_{\text{b, Rd}} = 1.5\, t d f_y/\gamma_{\text{M0}}$	(4)
Bearing resistance of plate and pin, additional requirement for replaceable pins	$F_{\text{b, Rd, ser}} = 0.6\, t d f_y/ \gamma_{\text{M6, ser}}$	(5)
Bending resistance of pin	$M_{\text{Rd}} = 1.5\, W_{\text{el}} f_{\text{yp}}/\gamma_{\text{M0}}$	(6)
Bending resistance of pin, additional requirement for replaceable pins	$M_{\text{Rd, ser}} = 0.8\, W_{\text{el}} f_{\text{yp}}/ \gamma_{\text{M6, ser}}$	(7)
Combined shear and bending resistance of pin	$\left[\dfrac{M_{\text{Ed}}}{M_{\text{Rd}}}\right]^2 + \left[\dfrac{F_{\text{v,Ed}}}{F_{\text{v,Rd}}}\right]^2 \leq 1$	(8)
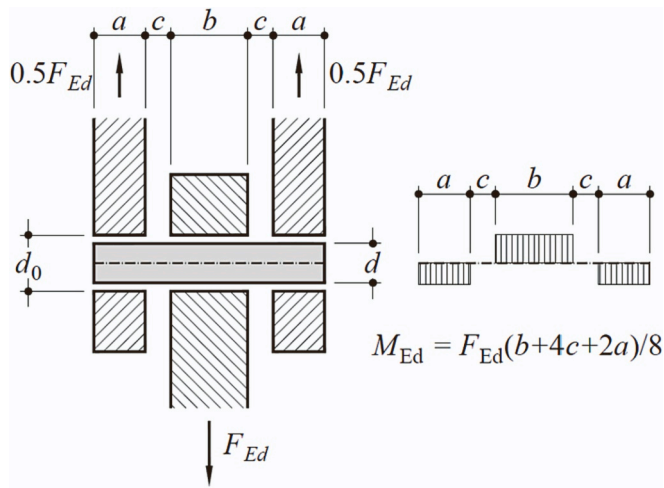
Fig. 4. Bending moment in a pin (adapted from Fig. 3.11 in EC3-1-8).

and dimensions $a = 8$ mm, $b = 12$ mm and $c = 5$ mm. The total pin length (within the connection) is 38 mm $< 3 \cdot d = 48$ mm. Therefore, according to clause 3.13.1(2) of EC3-1-8, it would be possible to design the pin as a bolt.

- Design as a bolt: the shear resistance of the pin should be calculated using Eq. (3) (as per Table 3.4 in EC3-1-8), whereupon $F_{v,Rd} = 49.2$ kN and $F_{Rd,bolt} = 2 \cdot F_{v,Rd} = 98.4$ kN.
- Design as a pin: the bending resistance is given by Eq. (6) as $M_{Rd} = 214$ kN·mm. Therefore, $F_{Rd,pin} = 8 \cdot M_{Rd}/(b + 4c + 2a) = 35.7$ kN.

The first value is 2.76 times the second one; choosing this first value as design resistance is clearly unsafe. Thus, clause 3.14.1(2) of EC3–1-8 results in an unsafe design and should be reconsidered.

4. Experimental program

4.1. Description of the prototypes

The analysed prototypes consist of circular hollow sections $\phi 120 \times 5$ welded to 15 mm thick end plates and double 10 mm thick lugs welded to the end plates. The cylindrical pins go through the holes of the four
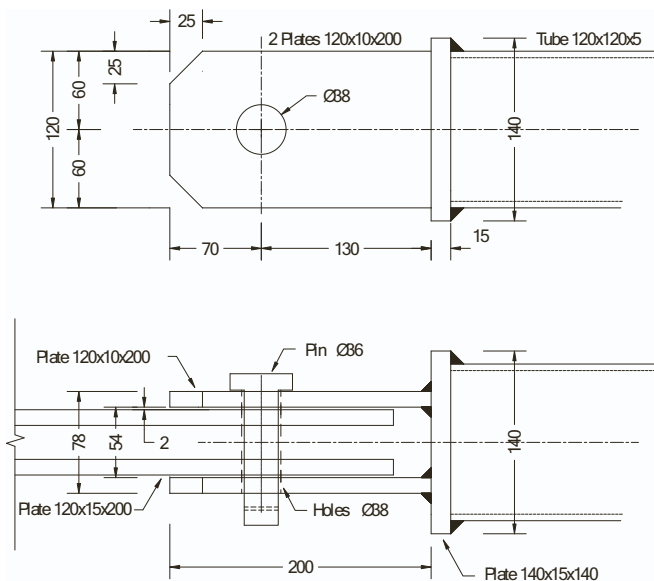
Fig. 5. Test model of the pin connection (Prototype 1).

lugs existing in two tube extremities (Fig. 5). This arrangement corresponds to a typical joint detail commonly used by PERI in scaffolding structures. All the models and coupons were fabricated by PERI.

The two tested models were similar, composed with the same materials (steel grade S275 for the plates and CK45 in pins). Prototype 1 has a 36 mm diameter pin ($d_0 = 38$ mm), while prototype 2 has a 20 mm diameter pin ($d_0 = 22$ mm). The geometry of the first model was established to represent a joint used in a real structure (as illustrated in Fig. 6); in the second model, a reduced pin diameter was used to force the failure mode to be the pin in bending. Prototypes 1 and 2 present a pin slenderness d/L (where L is the pin length within the connected parts) of 2.06 and 3.70, respectively. Thus, according to EC3–1-8, the pin in Prototype 1 could be designed as a bolt. Table 2 indicates the nominal and measured (average) geometrical dimensions of the prototypes.

4.2. Mechanical properties of materials

For each grade, the material properties of the steel plates and pins were determined from standard uniaxial tensile tests, according to EN 10002–1 [31], as illustrated in Figs. 7 and 8. The deformation of the coupons in the tensile tests was measured by electrical strain gauges with high strain capacity (10 to 15%, according to manufacturer information). According to EN 10002–1, the following properties were determined: yield strength, yield strain, tensile strength, failure strain and modulus of elasticity. They are summarized in Table 3. The steel grades used in 10 mm and 15 mm thick plates display a ductile behaviour, with a yield plateau and a large strain at failure. The steel used in the 20 mm pin also displays a ductile behaviour, with a yield plateau and a mean strain at failure of 13.28%; however, the 36 mm diameter pin steel exhibits different behaviour, without yield plateau and smaller yield and tensile strengths, as described in Table 3 and Fig. 8. For this material, the yield point has been found at the 0.2% residual strain point. The Young modulus displays expected values, between 208.7 and 222.5 GPa, for all steel qualities.

4.3. Test setup and instrumentation

The experimental tests were carried out on a universal test machine at the Steel Structures Laboratory of the Civil Engineering Department of the University of Coimbra (Fig. 9). The tests include several loading and unloading cycles until failure, performed with displacement rates of 0.01 mm/s and 0.05 mm/s in the elastic and plastic range, respectively. The two prototypes were instrumented with electrical strain gauges (linear and rosettes) and displacement transducers (LVDTs) as illustrated in Fig. 10. The tensile forces were applied through 20 mm thick plates. Besides the strain gauges glued to the connecting plates, two strain gauges were applied on the pins on diametral opposite sides to assess the flexural strains. Finally, to evaluate the global deformation of the prototypes, two displacement transducers were also placed (CH001 and CH002).

4.4. Description of tests and result analysis

4.4.1. Prototype 1: $\phi 36$ mm pin

For prototype 1, failure occurred for a tensile force of 627.5 kN, mostly because of the crushing of the 10 mm thick plates, with progressive ovalization of the holes. Additionally, the pin also exhibited significant plastic flexural deformation, forcing the connecting plates to bend laterally (Fig. 11). The force-displacement relation for the whole prototype is shown in Fig. 12, where it is noted that yielding started at approximately 300 to 350 kN, failure occurring after extensive deformation, for a displacement slightly over 20 mm. Fig. 13 illustrates the force-strain curves taken (i) along the critical transverse section of the 10 mm plate (strain gauges CH007, CH008 and CH009) and (ii) in front of the pin (strain gauges CH013 and CH014). It clearly shows that the
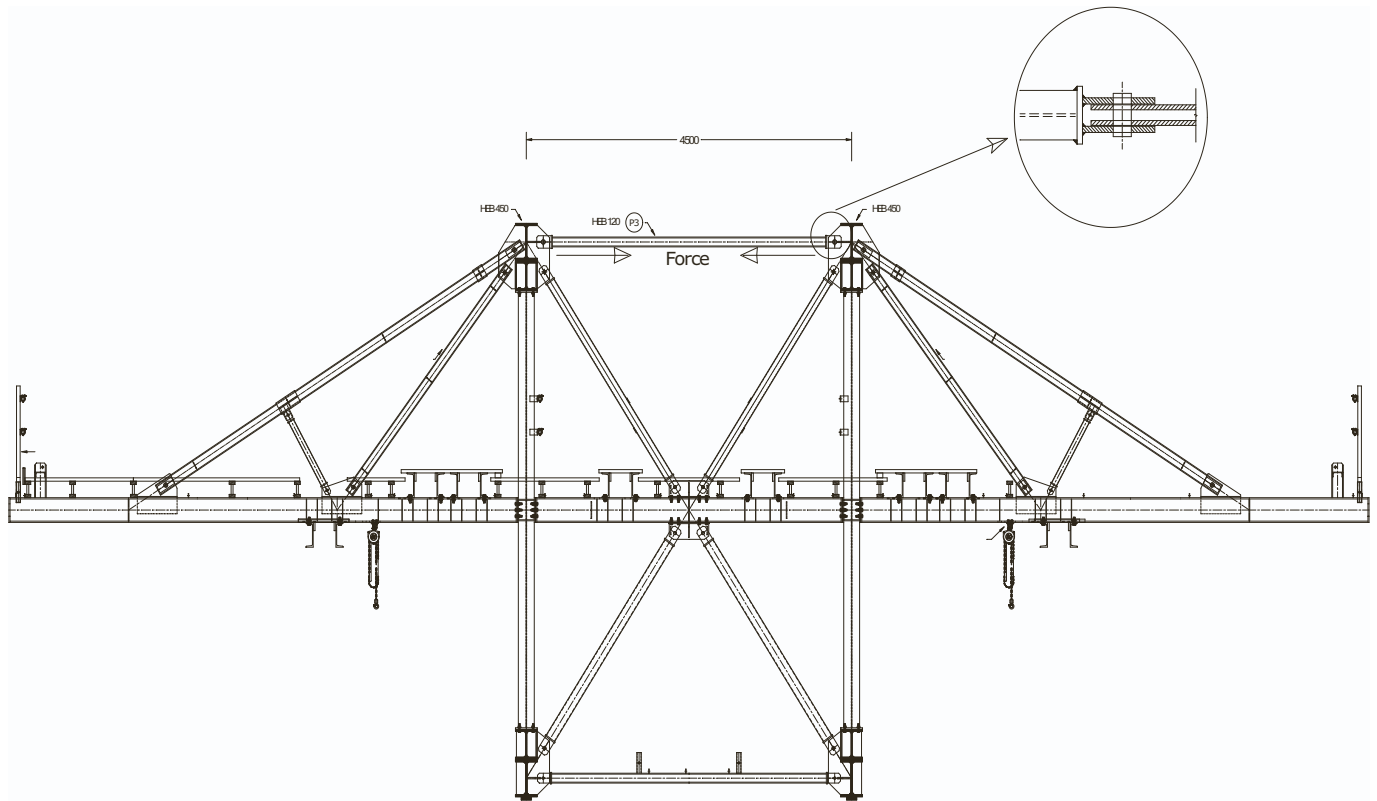
Fig. 6. Use of tested pin connections in temporary structures.

Table 2
Geometrical characterization of the connecting elements.

Element	Dimension	Prototype			
		P1 (φ36mm)		P2 (φ20mm)	
		Real	Nominal	Real	Nominal
10 mm plate	Width (mm)	120.5	120	121.3	120
	Thickness (mm)	10.1	10	10.1	10
	Hole diameter (mm)	36.8	38	21.4	22
15 mm plate	Width (mm)	120.6	120	120.9	120
	Thickness (mm)	15.0	15	15.0	15
	Hole diameter (mm)	36.7	38	21.3	22
Pin	Diameter (mm)	35.8	36	19.8	20

first zone to yield is in front of the pin (CH013); in this area, the compressive strain exceeded the yield strain (of the order of 1870 με according to Table 3), for a tensile force of 250 kN. For a tensile force of 400 kN, the stress concentration area next to the hole (CH009) also yielded in tension. Finally, for a tensile force slightly over 500 kN, complete yielding of the transverse cross-section was noted (CH007 and

CH008), as well as complete yielding in compression in front of the pin (CH014). The strain gauges at the back of the 10 mm plates (CH003 to CH006), as well as the strain gauges glued to the 15 mm plates never reached yield. To evaluate the behaviour of the pin, consider Fig. 14, which represents strains at two opposite sides of the pin, roughly halfway between the plates. It is noted that yielding started at a relatively low value of 300 kN, thus also contributing to the failure of the connection.

4.4.2. Prototype 2: φ20 mm pin

For Prototype 2, failure occurred for a tensile force of 214.1 kN, mostly the caused by complete yielding of the pin in bending, illustrated in Fig. 15. In contrast to Prototype 1, Prototype 2 exhibited some initial geometrical imperfections, namely with respect to symmetry and parallelism of the plates. The force-displacement relation for Prototype 2 is shown in Fig. 16, where it is noted that plasticity starts at about 50 to 60 kN. For this prototype, all strain gauges installed on the 10 mm and 15 mm plates did not yield. Conversely, the strain gauges glued to the pin show that the pin started yielding in bending at a tensile force of about 60 kN (Fig. 17), thus coinciding with the global yielding of the
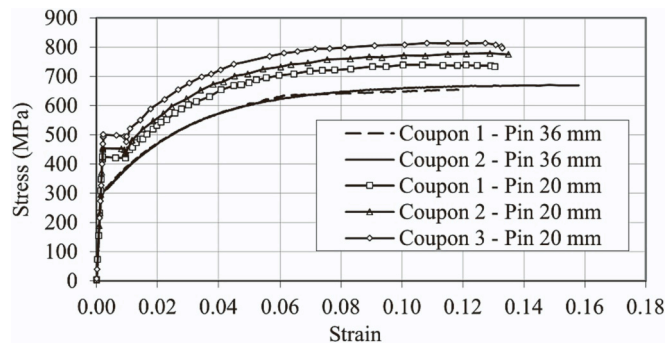

Fig. 7. Steel coupons.

Fig. 8. Stress-strain curves for steel of pins.

Table 3
Mechanical properties of materials.

Coupons		Yield strength (MPa)	Yield strain (%)	Tensile strength (MPa)	Failure strain (%)[b]	Young Modulus (GPa)
φ36mm pin	1	321.01[a]	0.152	670.52	11.79	211.4
	2	321.30[a]	0.149	671.16	15.80	215.4
	Avg.	321.16	0.151	670.84	13.80	213.4
φ20mm pin	1	421.21	0.190	739.45	13.05	221.7
	2	452.06	0.205	779.57	13.50	220.0
	3	497.91	0.224	813.92	13.30	222.5
	Avg.	457.06	0.206	777.65	13.28	221.4
10 mm plate	1	393.20	0.188	696.10	9.12	208.7
	2	383.30	0.180	694.96	11.88	212.7
	3	409.32	0.194	721.18	19.60	210.6
	Avg.	395.27	0.187	704.08	13.53	210.7
15 mm plate	1	430.31	0.201	707.08	15.74	214.4
	2	429.36	0.204	709.32	21.22	210.9
	3	422.10	0.192	703.13	22.60	220.4
	Avg.	427.26	0.199	706.75	19.85	215.2

[a] Stress corresponds to a residual strain of 0.2% since steel does not display a yield plateau.
[b] Strain at maximum capacity of strain gauges; in some coupons, the ultimate strain was larger.
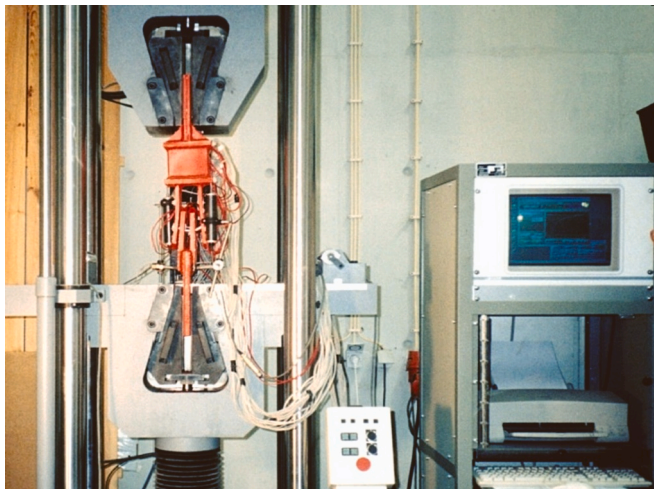
Fig. 9. Test setup.

prototype. Even though the main failure mode was by complete yielding of the pin in bending, at a force of about 1.7×60 kN = 102 kN (where 1.7 corresponds to the shape factor of a circular section), another failure mechanism developed, the pin working in shear until a final failure force of 214.1 kN.

4.5. Comparative analysis with code provisions

For pin connections, with the geometry of the plates in accordance with the dimensional requirements given in Table 3.9 of EC3–1-8, the code provisions for the design of plates and pins, already described in Table 1, consist of (i) shear resistance of the pin ($F_{v,Rd}$), (ii) bearing resistance of the plates and pin at serviceability ($F_{b,Rd,ser}$) and ultimate limit ($F_{b,Rd}$) states, (iii) bending resistance of the pin at serviceability ($F(M_{Rd,ser})$) and ultimate limit ($F(M_{Rd})$) states and, (iv) combined shear and bending resistance of the pin ($F(M_{Rd}, F_{v,Rd})$).

Based on the actual mechanical properties and geometrical dimensions, the resistance of the various failure modes was evaluated according to the codes, with and without partial coefficients, and are listed in Table 4.

Examination of the results for prototype 1 reveals that the governing failure mode is bearing ($F_{b,Rd}$ = 347.9 kN), the bending resistance is slightly higher ($F(M_{Rd}, F_{v,Rd})$ = 358.4 kN). It is noted that these values match the experimental results since the connection started to yield at an applied force in the interval 300–350 kN. Figs. 18-20 compare the experimental results with the code predictions for the relevant failure modes.

Concerning bearing on the 10 mm plate, Fig. 19 shows that, at the code resistance level for this failure mode ($F_{b,Rd}$ = 347.9 kN), hardly any yielding occurred around the bolt hole, with only some localised yielding in front of the hole (strain gauge CH013). At this level of applied force, the total deformation of the prototype was approximately 2.0 mm (Fig. 18), a value that also includes some initial adjustments to eliminate slack. Concerning the pin, the experimental force-strain curves of Fig. 20 show that yielding in bending started at around 300 kN, slightly below the code resistance of $F(M_{Rd}, F_{v,Rd})$ = 358.4 kN.

For prototype 2, bending and shear of the pin (bending dominant) is the critical failure mode. EC3–1-8 yields $F(M_{Rd}, F_{v,Rd})$ = 91.4 kN. That accurately matches the experimental results, as depicted in Figs. 21-22. The analytical resistance for bearing of the pin and plate ($F_{b,Rd}$ = 237.4 kN) and shear resistance of the pin ($F_{v,Rd}$ = 286.8 kN) are higher than the failure load of the joint (214.1 kN), a conclusion that is also matched by the experimental observations.

5. Parametric study

The simple counterexample presented in Section 3 has shown that the possibility to design a pin as a bolt whenever the length of the pin is <3 times the diameter of the pin should be eliminated because the resistance of the pin (Eqs. (6) and (8)) is lower (sometimes much lower) than the resistance of a bolt having the same geometrical and material characteristics.

A systematic parametric study on a large sample of pin connections that satisfy the above indicated geometrical condition was carried out to identify the proportion of cases that exhibit lower resistance of the pin when compared to its resistance as a bolt, based on the design expressions in EC3–1-8. The pin diameters considered are 12 mm, 16 mm, 20 mm, 24 mm, 30 mm and 36 mm; three-plate and four-plate configurations were studied. Different realistic combinations of lug thicknesses and gaps were considered (with the total pin length within the connection always satisfying $L < 3d$). S355 was assumed as pin material. For each case, the design resistance $F_{Rd,bolt}$ (design as a bolt) was compared to the design resistance $F_{Rd,pin}$ (design as a pin). 11,249 cases were considered in total. 10,324 cases (91.78% of the total) showed $F_{Rd,bolt} > F_{Rd,pin}$, with a ratio $F_{Rd,bolt}/F_{Rd,pin}$ ranging from 1 to 3.98, a mean value of 2.09 and a c.o.v of 28.2% and were, therefore, inadequate based on the code specifications. This supports the recommendation to eliminate the possibility to design a pin as a bolt.

6. Proposed design model

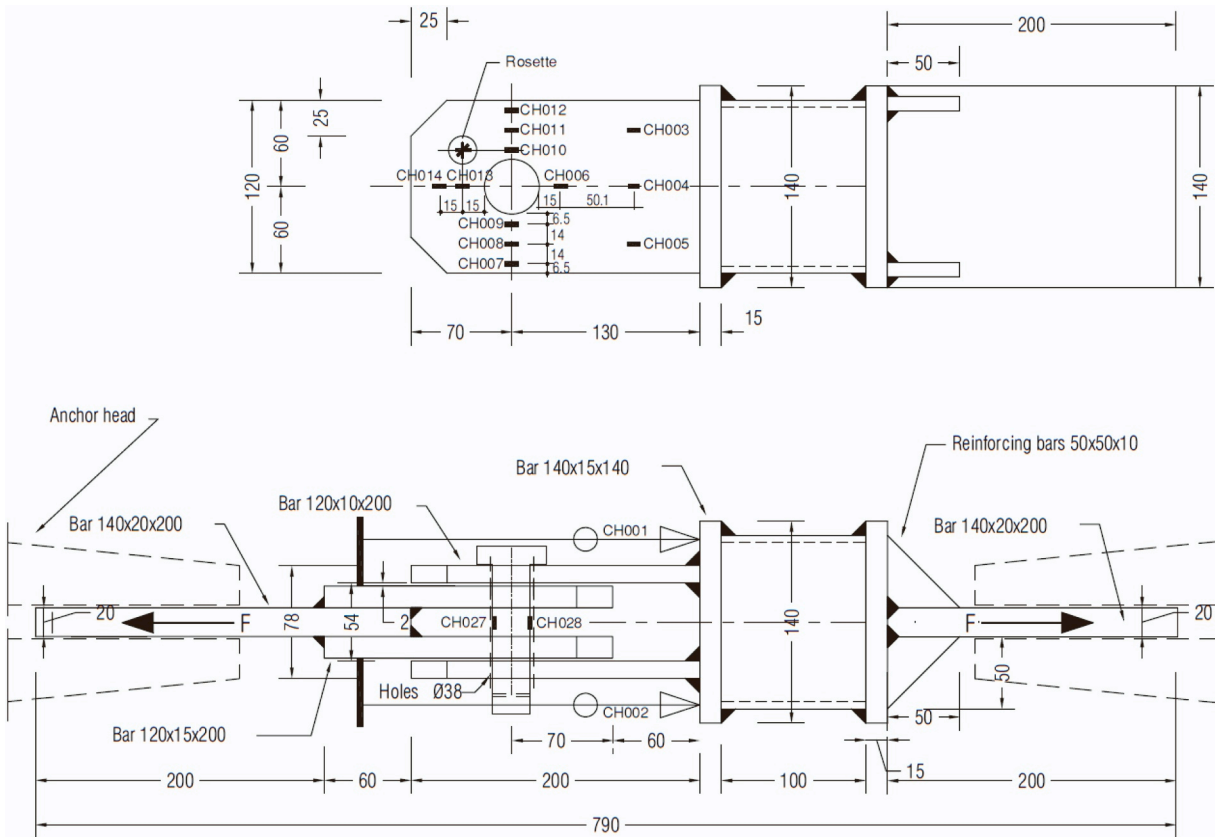The current provisions of EC3–1-8 for pin connections consider only

Fig. 10. Instrumentation of the laboratory models: exemplification for Prototype 1 with φ36mm pin.

(a)   (b)

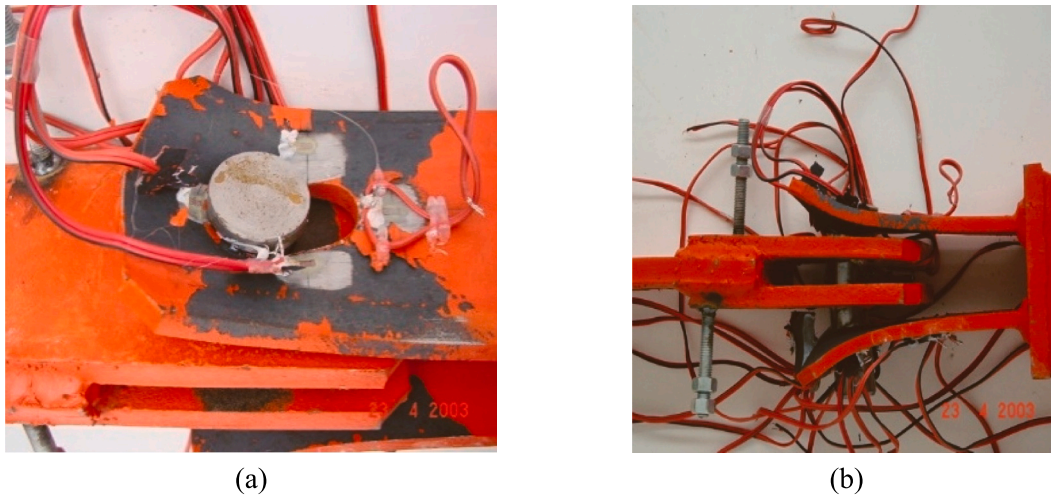**Fig. 11.** Prototype 1 with φ36mm pin after failure: (a) plate bearing; (b) pin and plate bending.

the possibility of the connection load acting symmetrically. However, the experiments described in Section 4 show that the existence of gaps between lugs, typical of this type of connection, results in the asymmetry of the assembly at the Ultimate Limit State. In this Section, a simple design model is developed to consider this asymmetry.

6.1. Internal forces at pins

A typical cross-section of a pin connection is shown in Fig. 23(a), having two supporting plates at both sides, a central loaded plate, and two retaining caps attached to the pin and in contact with the edge

plates. No detailed rules are currently given for such caps in EC3–1-8, so it will be assumed that they have no capacity to rotationally restrain the pin (contrary to, say, the washer and nut in a bolt assembly properly tightened).

The dimensional limits for the plate geometry (edge distance, position of the hole, plate thickness) are given in Table 3.9 of the cited standard and are not discussed here. An idealized model of the pin connection is shown in Fig. 23(b), as currently adopted in EC3–1-8 (cf. clause 3.13). Internal forces on the pin are calculated using simple beam theory, assuming all forces applied as uniformly distributed along the length in contact on each part (as per clause 3.13.2(2) of the standard).
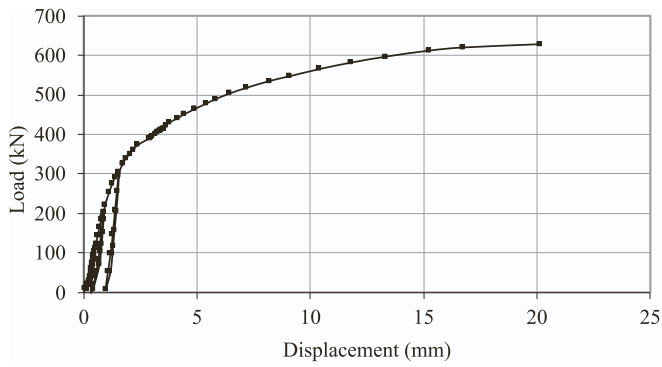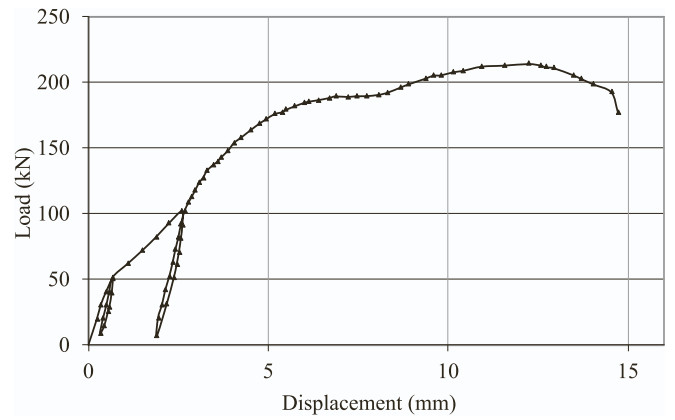
Fig. 12. Force-displacement curve for Prototype 1.
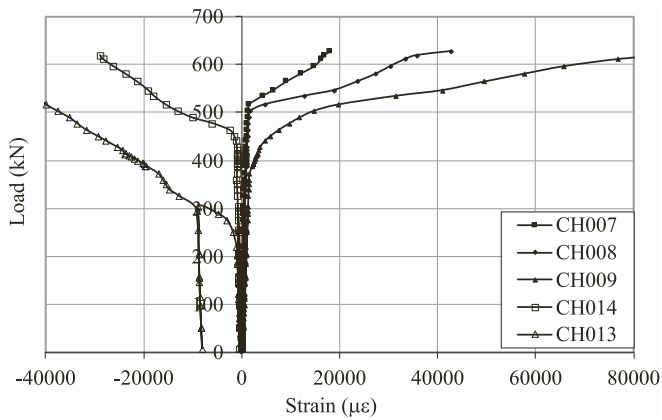

Fig. 13. Force-strain curves on 10 mm plate of Prototype 1.

Fig. 14. Force-strain curves on the pin of Prototype 1.
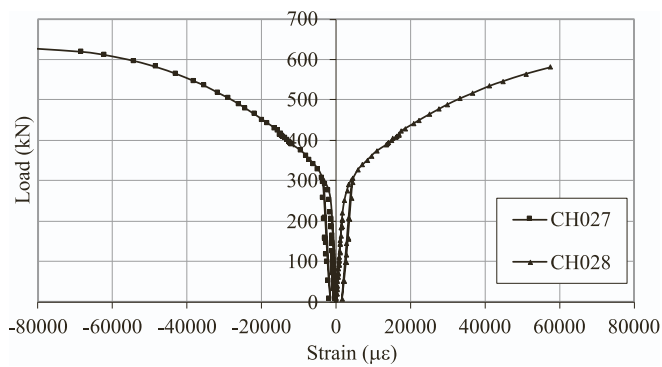

Fig. 15. Prototype 2 after failure.

Fig. 16. Force-displacement curve for Prototype 2.

Fig. 17. Force-strain curves for pin of Prototype 2.

Table 4
Resistance of the connection components.

Prototype		$F_{v,Rd}$ (kN)	$F_{b,Rd}$ (kN)	$F(M_{Rd})$ (kN)	$F(M_{Rd},F_{v,Rd})$ (kN)
P1	$\gamma = 1.0$	808.1	**347.9**	399.9	358.4
(ϕ36mm)	γ code	646.5	**278.3**	399.9	340.8
P2	$\gamma = 1.0$	286.8	237.4	96.4	**91.4**
(ϕ20mm)	γ code	229.4	189.9	96.4	**88.9**
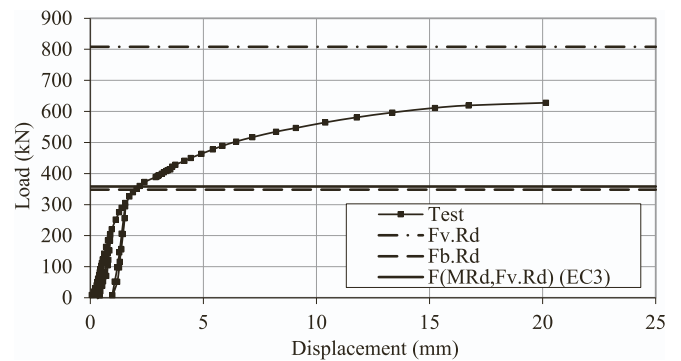
Fig. 18. Comparison between the experimental force-displacement curve and EC3–1-8 code resistance, Prototype 1.

The maximum bending moment on the pin occurs at the central section of the idealized beam. The force applied in the loaded plate (central plate) is equally distributed in two reactions on the supporting plates (lateral plates); therefore, the shear force diagram is antisym-
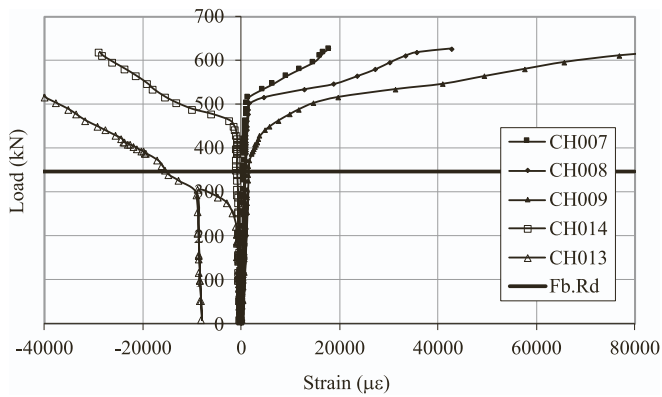
Fig. 19. Comparison between the experimental force-strain curve and EC3–1-8 code resistance for 10 mm plate, Prototype 1.
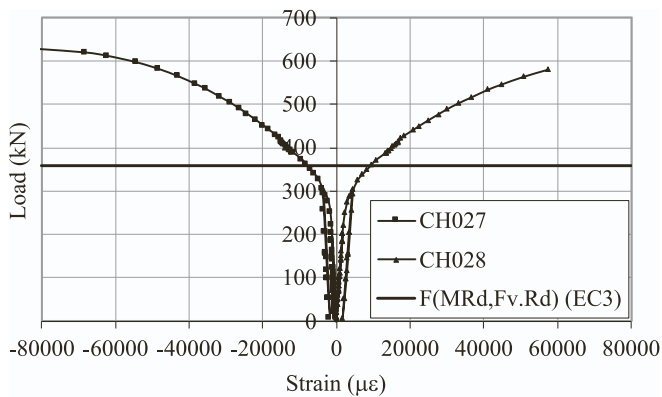

Fig. 20. Comparison between experimental force-strain curve and EC3–1-8 code resistance for the pin, Prototype 1.
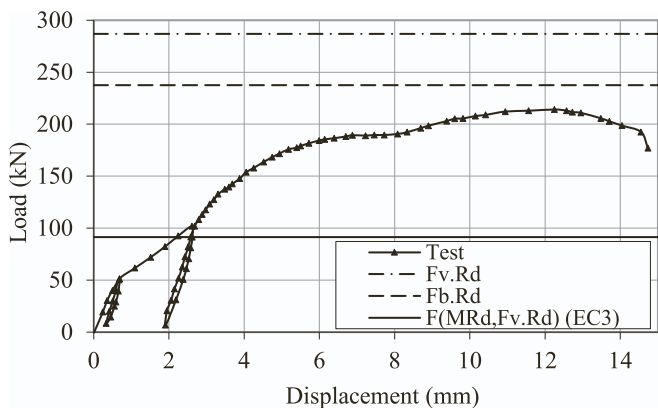

Fig. 21. Comparison between the experimental force-displacement curve and EC3–1-8 code resistance, Prototype 2.

metric, the bending moment diagram is symmetric, and the maximum values can be calculated with simple beam theory. Two significant cross-sections are identified: Section B (or D), where the maximum shear force concurs with a significant bending moment, and section C, with the maximum bending moment and no simultaneous shear force. The corresponding internal forces are
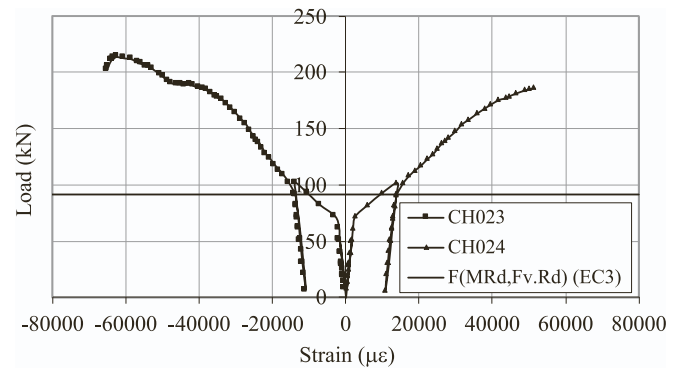
$$F_{v,B,sym} = \frac{F}{2}, \tag{9}$$

Fig. 22. Comparison between the experimental force-strain curve and EC3–1-8 code resistance for the pin, Prototype 2.
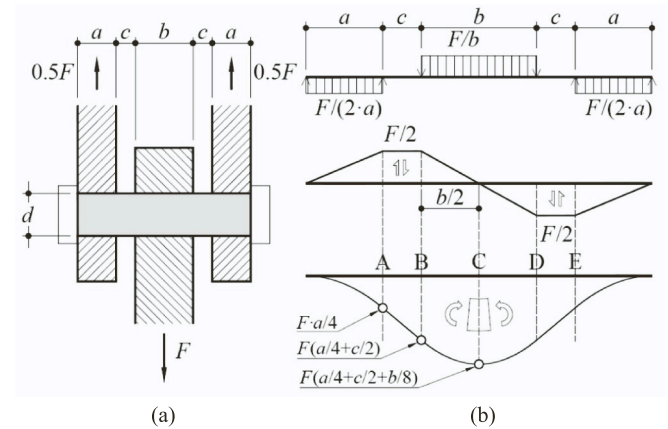

Fig. 23. Pin connection, symmetrical situation: (a) cross-section; (b) idealized beam model.

$$M_{B,sym} = \frac{F}{4}(a + 2c), \tag{10}$$

$$M_{C,sym} = \frac{F}{8}(2a + b + 4c). \tag{11}$$

Moment-shear interaction should be checked at all cross-sections between B and C.

If the plates are not locked (for instance, by washers) the position of the central plate with respect to the supporting plates cannot be secured. The worst-case scenario is shown in Fig. 24(a), where the central plate has slid totally towards one side; it is assumed that the retaining caps prevent further movement of the central plate. Reactions on the supporting plates are no longer equal, but can easily be found using simple equilibrium considerations as αF (maximum reaction, right support on figure) and $(1-\alpha)F$ (minimum reaction, left support on the figure), where

$$\alpha = \frac{a + b + 4c}{2a + 2b + 4c} \geq 0.5, \tag{12}$$

whereupon the values of shear and bending moment in three critical locations B, C, D, can be determined, as shown in Fig. 24(b). The following equations are derived:

$$F_{v,B,asym} = F(1 - \alpha), \tag{13}$$

$$M_{B,asym} = F(1 - \alpha)\left(\frac{a}{2} + 2c\right), \tag{14}$$
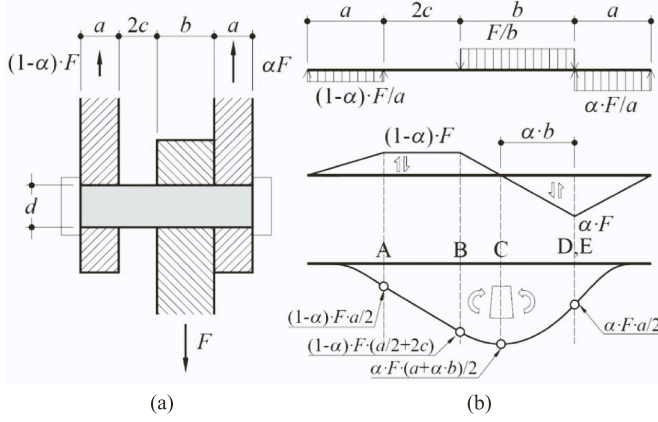
$$F_{v,C} = 0, \tag{15}$$

Fig. 24. Pin connection, asymmetrical situation: (a) cross-section; (b) idealized beam model.

$$M_{C,asym} = F\frac{\alpha}{2}(a + \alpha b), \tag{16}$$

$$F_{v,D,asym} = \alpha F, \tag{17}$$

$$M_{D,asym} = F\frac{\alpha}{2}a. \tag{18}$$

In these expressions subscript '*asym*' indicates the asymmetrical situation, as opposed to the symmetrical situation treated above. Every cross-section of the pin between B and D should be checked for moment-shear interaction.

6.2. Pin verification

This section deals only with the pin resistance and does not include the verification of the bearing capacity of plates or contact stress limitation, which should be carried out independently. Verification depends on the need for future replacement of the pin, which requires comparatively lower deformations; in EC3-1-8 this is achieved through a more restrictive limit on the pin stress.

The strict verification for non-replaceable pins is:

$$U_{nrp} = max\left\{\frac{M_{Ed}}{M_{Rd}}; \frac{F_{v,Ed}}{F_{v,Rd}}; \left(\frac{M_{Ed}}{M_{Rd}}\right)^2 + \left(\frac{F_{v,Ed}}{F_{v,Rd}}\right)^2\right\} \le 1, \tag{19}$$

where U_{nrp} is the utilization factor, subscript 'nrp' stands for 'non-replaceable pin', and all other variables have been introduced in previous sections. The check should be performed (in theory) for both symmetrical and asymmetrical layouts and at all cross-sections across the pin axis, although the practical range is limited to points between B and D. Additional verification for bearing should be performed.

The strict verification for replaceable pins is:

$$U_{rp} = max\left\{U_{nrp}; \frac{M_{max,Ed,ser}}{M_{Rd,ser}}\right\} \le 1, \tag{20}$$

where $M_{max,Ed,ser}$ is the maximum bending moment (section C) at SLS, and subscript 'rp' stands for 'replaceable pin'; no shear interaction check is required for SLS. Additional verifications for bearing and contact stress should be performed.

6.3. Utilization factors

As indicated above, for non-replaceable pins the strict verification given by Eq. (19) must be performed for both the symmetrical and asymmetrical situations. Thus, two different utilization factors can be defined, namely

$$U_{sym} = max\left\{\begin{array}{l} U_{sym,M} = \dfrac{M_{Ed,sym}}{M_{Rd}} \\[2mm] U_{sym,V} = \dfrac{F_{v,Ed,sym}}{F_{v,Rd}} \\[2mm] U_{sym,M+V} = \left(\dfrac{M_{Ed,sym}}{M_{Rd}}\right)^2 + \left(\dfrac{F_{v,Ed,sym}}{F_{v,Rd}}\right)^2 \end{array}\right\}, \tag{21}$$

$$U_{asym} = max\left\{\begin{array}{l} U_{asym,M} = \dfrac{M_{Ed,asym}}{M_{Rd}} \\[2mm] U_{asym,V} = \dfrac{F_{v,Ed,asym}}{F_{v,Rd}} \\[2mm] U_{asym,M+V} = \left(\dfrac{M_{Ed,asym}}{M_{Rd}}\right)^2 + \left(\dfrac{F_{v,Ed,asym}}{F_{v,Rd}}\right)^2 \end{array}\right\}, \tag{22}$$

$$U = max\{U_{sym}; U_{asym}\}. \tag{23}$$

The largest utilization factor among U_{sym} and U_{asym} indicates the critical design situation (symmetrical, asymmetrical). The proportion between U_{sym} and U_{asym} is examined hereby by means of the following parametric study: for a given thickness $b = 40$ mm of the loading plate, the thickness of the supporting plates a is varied in the range $[b/2, b]$; the clear space c is defined as $c = b$-a, therefore the total length of the pin is always constant and equal to $3b$. For every combination $[b, a, c]$, the pin diameter d is varied between $b/2$ (= 20 mm) and $6b$ (= 240 mm). The applied force F_{Ed} is adjusted so that $U = 1$ (within a numerical tolerance of 1/10000). Then the ratio U_{sym}/U_{asym} is found. The study is repeated for two different typical pin materials, 42CrMo4 + QT and S355J2. Results for 42CrMo4 + QT are shown in Fig. 25(a), whereas results for S355J2 are shown in Fig. 25(b). The material properties indicated in the plot labels are the nominal values, corresponding to small thickness (up to 16 mm for S355J2, up to 40 mm for 42CrMo4 + QT), but the properties used in the study were determined according to the pin diameter as per EN 10025–2 [32] for S355J2 or EN 10083–3 [33] for 42CrMo4 + QT; the abrupt change in material properties as a function of thickness indicated in both standards is the reason of the jagged shape in the curves. The bottom part of each figure shows the failure mode for each combination of geometrical parameters. The variable in the horizontal axis is the pin slenderness λ (ratio of pin length $2a + b + 2c$ to pin diameter d).

For both materials, Fig. 25 shows two different regions in the curves:

- Region 1, starting from the left, corresponds to stout pins with small slenderness (approx. $\lambda < 1.1$ to 1.5) for which the asymmetrical situation is more critical. The failure mode is by combination of moment and shear (cross-section D in Fig. 24).
- Region 2, correspond to pins with moderate to large slenderness (approx. $\lambda > 1.1$ to 1.5), for which the symmetrical situation prevails. The failure mode is always by pure moment (cross-section C in Fig. 23).

The dependence of utilization factors on pin slenderness λ is shown in Fig. 26, where the different terms inside the bracket in Eqs. (21) and (22) are plotted versus λ. The trends in both plots are similar and demonstrate the previous statements, that is:

- In region 1 (stocky pins) the asymmetrical verification for interaction between bending moment and shear force dominates the design.
- In region 2 (slender pins) the symmetrical verification for bending moment dominates the design. Interaction with shear is not relevant.
- Shear verification alone is never critical

Applying these three observations, the following condition can be established for $U_{sym} = U_{asym}$:
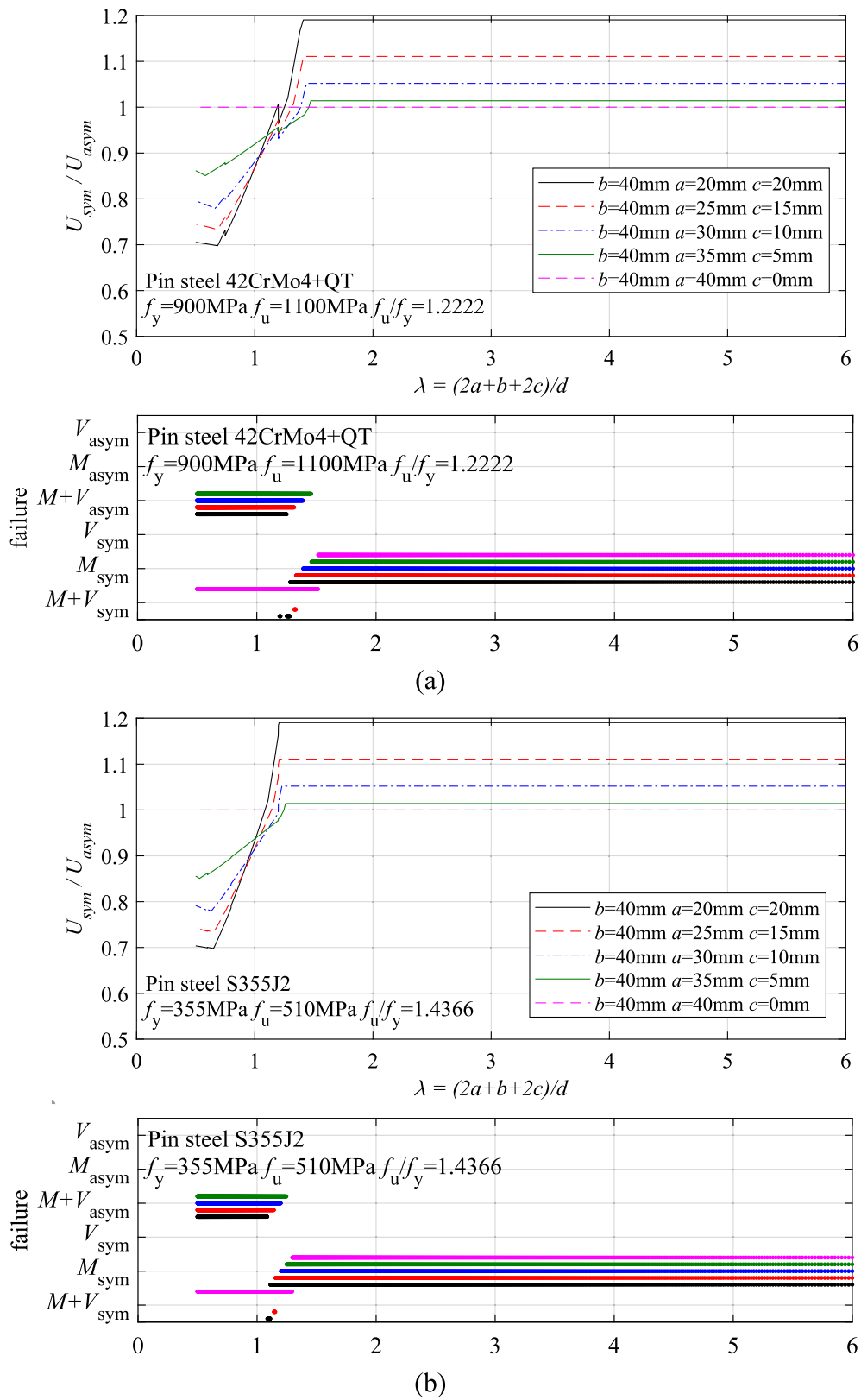
Fig. 25. Prevalence of strict symmetrical or asymmetrical verification for two different pin materials: (a) 42CrMo4 + QT Pin; (b) S355J2 Pin.
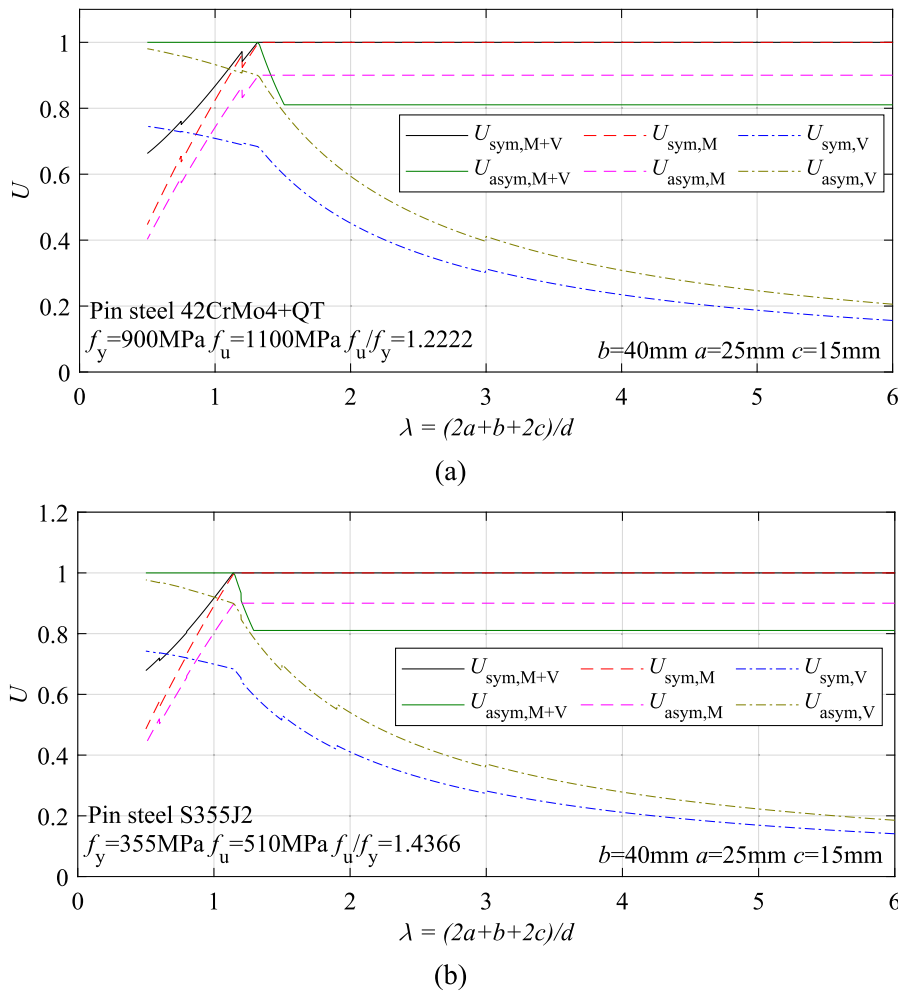
Fig. 26. Dependence of utilization factors from slenderness for a typical geometric configuration and two different pin materials: (a) 42CrMo4 + QT Pin; (b) S355J2 Pin.

$$\left(\frac{M_{C,sym,Ed}}{M_{Rd}}\right)^2 = \left(\frac{F_{v,D,asym,Ed}}{F_{v,Rd}}\right)^2 + \left(\frac{M_{D,asym,Ed}}{M_{Rd}}\right)^2. \tag{24}$$

Using Eqs. (3), (6), (11), (12), (17) and (18), this expression transforms to:

$$\left(F_{Ed}\frac{32}{12}\frac{(2a+b+4c)}{\pi d^3}\frac{\gamma_{M0}}{f_{y,pin}}\right)^2 = \cdot\left(F_{Ed}\frac{20}{3}\frac{\alpha}{\pi d^2}\frac{\gamma_{M2}}{f_{u,pin}}\right)^2 + \left(F_{Ed}\frac{32}{3}\frac{\alpha a}{\pi d^3}\frac{\gamma_{M0}}{f_{y,pin}}\right)^2, \tag{25}$$

and, after some manipulation, the following relationships are derived:

$$d_{lim} = \frac{2}{5}\frac{f_{u,pin}}{f_{y,pin}}\frac{\gamma_{M0}}{\gamma_{M2}}\frac{\sqrt{(2a+b+4c)^2 - 16a^2\alpha^2}}{\alpha}; \tag{26}$$

$$\lambda_{lim} = \frac{2a+b+2c}{d_{lim}}. \tag{27}$$

This is the limiting condition for which the asymmetrical (stocky pins, $\lambda < \lambda_{lim}$, $d > d_{lim}$) or symmetrical (slender pins, $\lambda > \lambda_{lim}$, $d < d_{lim}$) verifications are, respectively, critical. Eq. (26) must be solved iteratively for given values of a, b, c, because the material properties ($f_{u,pin}$, $f_{y,pin}$) are dependent on d_{lim}. A good initial value to iterate is $d_{lim} = 2a + b + 2c$, that is, $\lambda_{lim} = 1$.

As an example, for $b = 40$ mm, $a = 25$ mm, $c = 15$ mm, from Eq. (12), $\alpha = 0.658$; for a 42CrMo4 + QT pin, iterative application of Eq. (26) leads to $d_{lim} = 91$ mm, or $\lambda_{lim} = 1.32$. This limiting value is evident in

Figs. 25(a) and 26(a). Likewise, for a S355J2 pin, $d_{lim} = 107$ mm or $\lambda_{lim} = 1.13$, as shown in Figs. 25(b) and 26(b).

The results of this study are in direct conflict with clause 3.13.1(2) of EC3–1-8, that allows pins to be calculated as bolts for slenderness λ below 3. Bending moment is shown to be always critical in design verifications, regardless of pin slenderness and/or consideration of asymmetry. In particular:

- The maximum bending moment in a typical pin configuration formed by a central load plate and two edge support plates with gaps in between is always given by the symmetrical configuration.
- The maximum shear force in the same configuration occurs when the central plate is totally asymmetrical. This shear concurs with a reduced bending moment.
- If the resistance formulae indicated by EC3–1-8 part 1–8 are used for the pin, the pin slenderness λ (ratio of pin diameter to pin length) is the parameter governing the strict design of the pin. A limiting value λ_{lim} is given by Eq. (27). Above this slenderness, only the symmetrical bending moment needs to be considered. Below this slenderness, asymmetrical interaction M-V is the critical verification.
- The study shows that clause 3.13.1(2) in the current EN 1993 Part 1–8 (design of pin as a bolt for slenderness below 3) is inadequate.

7. Conclusions

This paper focuses on pin connections, and more particularly on

certain design specifications included in the current version of EN 1993 Part 1–8. The paper includes a literature review, experimental tests, analytical derivations and two parametric studies. From the material presented, the following relevant conclusions are drawn:

1. Numerous studies on pin connections exist. However, most of them deal with the lugs and very few tackle the pin itself. In addition, the configurations studied are mostly in tension, and do not correspond well with current engineering practice.
2. A need for further experimentation in this field is evident. Some open research issues are design rules for complex geometries and load situations; proper characterization of pin strength and stiffness; use of high-strength steel in lugs; pin connections with >3 lugs; characterization of rotation capacity; pin connections in compression.
3. The EC3–1-8 proposal for design of pin connections is very limited in scope and does not really cover current engineering situations. Important issues are not included in design verifications (plate dishing, effect of hole clearances, retainer elements, accidental asymmetry of the connection, etc). Design of pins for Ultimate Limit State according to EC3-1-8 might result in large yielding at Serviceability Limit State, for which no deformation check is included.
4. Clause 3.13.1(2) in the current EC3–1-8 states that the pin may be designed as a bolt if its slenderness is below 3. This Clause has been found to be unsafe.
5. The potential asymmetry of the pin connection, which is possible due to gaps between plates, must be considered in the design. For a 3-plate pin connection with given geometry and pin material, a slenderness limit λ_{lim}, Eq. (27), exists that separates stocky pins from slender pins. For slender pins, the bending moment in the symmetrical situation is critical. For stocky pins, moment-shear interaction in the asymmetrical situation is critical

Author contribution credit statement

Luís Simões da Silva: Validation, Methodology, Conceptualization, Writing - Original Draft, Review & Editing. Jorge Conde: Investigation, Validation, Methodology, Writing - Original Draft, Review & Editing. Trayana Tankova: Investigation, Validation, Methodology, Writing - Review & Editing. Rui Simões: Investigation, Validation, Methodology, Writing - Review & Editing, Tiago Abecasis: Validation, Conceptualization, Writing - Review & Editing. All authors discussed the results and contributed to the final manuscript.

Acknowledgment and funding sources

Declaration of Competing Interest

The authors declare that they have no known competing financial interests or personal relationships that could have appeared to influence the work reported in this paper.

Data availability

Data will be made available on request.

References

[1] European Committee for Standardization (CEN), EN-1993-1-8 – Eurocode 3: design of steel structures – Part 1–8: design of joints, 2005.
[2] F. Bohny, Theorie und Konstruktion versteifter Hängebrücken, W. Engelmann, Leipzig, 1905.
[3] M.A. Melcon, F.M. Hoblit, Developments in the analysis of lugs and shear pins, Prod. Des. Eng. 24 (1953) 60–170.
[4] J.C. Ekvall, Static strength analysis of pin-loaded lugs, J. Aircr. 23 (5) (1986) 438–443, https://doi.org/10.2514/3.45326.
[5] H. Hertz, Über die Berührung fester elastischer Körper, J. Reine Angew. Mathem. 92 (156–171) (1882) 22.
[6] M.M. Frocht, H.N. Hill, Stress-concentration factors around a central circular hole in a plate loaded through pin in the hole, Am. Soc. Mech. Eng. 62 (1) (1940) A5–A9, https://doi.org/10.1115/1.4008987.
[7] S. Timoshenko, J.N. Goodier, Theory of Elasticity, McGraw-Hill, New York, 1951.
[8] R.N. Tolbert, R.M. Hackett, Experimental investigation of lug stresses and failures, AISC Eng. J. 11 (2) (1974) 34–37.
[9] R.S. Whitehead, A.J. Abbey, M.G. Glen-Bott, Analytical determination of stress intensity factors for attachment lugs. Rep. SON(P) 199, British Aerospace, Aircraft Group, Warton Division, Warton, England, 1978.
[10] A.K. Rao, Elastic analysis of pin joints, Comput. Struct. 9 (2) (1978) 125–144, https://doi.org/10.1016/0045-7949(78)90131-1.
[11] V.A. Eshwar, Analysis of clearance fit pin joints, Int. J. Mech. Sci. 20 (8) (1978) 477–484, https://doi.org/10.1016/0020-7403(78)90045-0.
[12] I. Harms, Pinned Connections, Master Thesis,, Delft University of Technology, The Netherlands, 2015.
[13] J. Montgomery, C. Higgins, J. Liu, Capacities of Pin and Hanger Assemblies Phase 1, No. CA18–3023, Oregon State University, 2018.
[14] B.G. Johnston, Pin-connected plate links, Trans. Am. Soc. Civ. Eng. 104 (1) (1939) 314–336, https://doi.org/10.1061/TACEAT.0005107.
[15] D. Duerr, G. Pincus, Pin clearance effect on pinned connection strength, J. Struct. Eng. 112 (7) (1986) 1731–1736, https://doi.org/10.1061/(ASCE)0733-9445(1986)112:7(1731).
[16] D. Duerr, G. Pincus, Deformation behavior of pinned connections with large pin clearance, J. Struct. Eng. 114 (12) (1988) 2803–2807, https://doi.org/10.1061/(ASCE)0733-9445(1988)114:12(2803).
[17] N.L. Pedersen, Stress concentration and optimal design of pinned connections, J. Strain Anal. Eng. Des. 54 (2) (2019) 95–104, https://doi.org/10.1177/0309324719842766.
[18] D. Duerr, Pinned connection strength and behaviour, J. Struct. Eng. 132 (2) (2006) 182–194, https://doi.org/10.1061/(ASCE)0733-9445(2006)132:2(182).
[19] W.D. Pilkey, D.F. Pilkey, Z. Bi, Peterson's Stress Concentration Factors, John Wiley & Sons, New Jersey, 2020.
[20] H.G. Luley, Pin-Connected Plates, BSCE Thesis,, Lehigh University, UK, 1942.
[21] G.T. Blake, Structural Tests of Large Pin-Connected Links, US Steel Research, Monroeville, Pa, 1981.
[22] D. Duerr, G. Pincus, Experimental Investigation of Pin Plates, Research Rep. No. UHCE 85–3, University of Houston, 1985.
[23] R.Q. Bridge, T. Sukkar, I.G. Hayward, M.V. Ommen, Behaviour and design of structural steel pins, Steel Compos. Struct. 1 (1) (2001) 97–110, https://doi.org/10.12989/scs.2001.1.1.097.
[24] C.O. Rex, W.S. Easterling, Behavior and modeling of a bolt bearing on a single plate, J. Struct. Eng. 129 (6) (2003) 792–800, https://doi.org/10.1061/(ASCE)0733-9445(2003)129:6(792).
[25] Y.S. Choo, K.C. Choi, K.H. Lee, The effects of eye bar shape and pin/hole tolerance on its ultimate strength, J. Constr. Steel Res. 26 (2–3) (1993) 153–169, https://doi.org/10.1016/0143-974X(93)90034-P.
[26] J. Vičan, M. Farbák, Analysis of high-strength steel pin connection, Civil Environ. Eng. 16 (2) (2020) 276–281, https://doi.org/10.2478/cee-2020-0027.
[27] P. Može, D. Beg, A complete study of bearing stress in single bolt connections, J. Constr. Steel Res. 95 (2022) 126–140, https://doi.org/10.1016/j.jcsr.2013.12.002.
[28] R.G. Scott, J.C. Stone, Effects of Design Variables on the Critical Stresses of Eye Bars under Load: An Evaluation by Photoelastic Modelling, No. UCRL-87071; CONF-820516-2, Lawrence Livermore National Lab, CA USA, 1982.
[29] A. Blake, Structural pin design, Des. News 29 (2) (1974) 88.
[30] J.M. Kulicki, Load factor design applied to truss members in design of greater new Orleans bridge no. 2, Transp. Res. Rec. 903 (1983).
[31] European Committee for Standardization (CEN), EN 10002–1 – Metallic Materials – Tensile Testing – Part 1: Method of Test at Ambient Temperature, 2001.
[32] European Committee for Standardization (CEN), EN 10025–2 – Hot Rolled Products of Structural Steels – Part 2: Technical Delivery Conditions for Non-Alloy Structural Steels, 2019.
[33] European Committee for Standardization (CEN), EN 10083–3 – Steels for quenching and tempering – Part 3: Technical delivery conditions for alloy steels, 2008.